Open Access
Inkwell Innovations in Life Sciences
ISSN: 3079-3335 (Print), 3079-3343 (Online)
https://inkwellliterature.com/index.php/lifescience
Volume: 2, Issue: 1, Pages: 52-72, Date Published: Jan 12, 2025

Research Article

Potential of Silver Nanoparticles in Phytoremediation of Wastewater and Their Effects on Growth Parameters of *Brassica campestris* L.

Asif Ahmad[1], Natasha Anwar[2], Sahar Nasim[3], Sania Shah[1], Sehrish Asad[1], Sirajuddin[1], Haleemullah[1], Shahzad Malak[4], Mohib Shah[1,*]

[1]Department of Botany, Abdul Wali Khan University Mardan, Pakistan
[2]Department of Chemistry, Abdul Wali Khan University Mardan, Pakistan
[3]Department of Botany, University of Malakand, Pakistan
[4]Marine Biotechnology, Faculty of Veterinary and Experimental Sciences, Catholic University of Valencia, Spain

***Corresponding Author**: Mohib Shah, Email: mohibshah@awkum.edu.pk

ABSTRACT

Innovative solutions that should be researched include using nanoparticles and plants to regenerate heavy metal-polluted water and soil effectively. Silver nanoparticles (AgNPs) synthesized and characterized from *Dryopteris filix* were employed in phytoremediation. Wastewater was collected from sewage water canals on the boundaries of Abdul Wali Khan University Mardan Garden Campus. There were 19 distinct physicochemical properties assessed. Hydroponic research was used to explore the effect of silver nanoparticles on plant growth, photosynthetic pigments, phytohormones, primary and secondary metabolites, antioxidant activity, CAT and POD, and chromium (Cr) accumulation in *Brassica campestris* L. In addition to the Cr-polluted medium supplemented with 50 mgL^{-1} of AgNPs, seedlings were cultivated in wastewater. An atomic absorption spectrophotometer (SPECTRO AAS-4000) was utilized to examine chromium in plant tissues. AgNPs improved plant growth and increased photosynthetic pigments, mitigating the stress of Cr and wastewater, while Cr and wastewater significantly reduced the development of seedlings. Plant growth, secondary metabolites, and phytohormones were all suppressed by chromium at a concentration of 50 mg L^{-1}. Production of phenol, flavonoids, indole acetic acid, protein, and sugar was increased, whereas oxidative stress was decreased in seedlings exposed to AgNPs. Chromium increased in wastewater application (131.4 & 82.2 mg kg^{-1}), whereas it dropped in AgNP application (104.6 & 82.2 $mgkg^{-1}$) in *B. campestris* root and shoot. These findings show that using the correct concentration of AgNPs can help plants remove heavy metals from polluted water through nano-phytoremediation.

Keywords: Nanoparticles, Cr phytoremediation, Wastewater, Physico-chemical parameters, Brassica campestris L., Hydroponic growth, Metabolites, Antioxidant enzymes

INTRODUCTION

Because of their high density or atomic weight, they are classified as heavy metals. In modern times, metallic chemical elements and metalloids that are hazardous to both humans and the environment are called "heavy metals." (Briffa et al., 2020). The environment is recognized to

be particularly threatened by toxic heavy metals including arsenic (As), cadmium (Cd), lead (Pb), copper (Cu), chromium (Cr), nickel (Ni), zinc (Zn), aluminum (Al), and manganese (Mn) among other contaminants (Ullah et al., 2015; Dhanarani et al., 2016; Karthik et al., 2017a). These heavy metals cause major health problems for ecosystems as well as for people (Zeraatkar et al., 2016; Chen et al., 2015; Ullah et al., 2015). Both organic and synthetic processes can release heavy metal contaminants into the environment, where they can end up in soil, water, or the atmosphere (Kuppusamy et al., 2017; Chen et al., 2015).

Due to its substantial toxicity, mutagenicity, and carcinogenicity, heavy metal contamination of the environment, particularly chromium (Cr), has lately become a major environmental concern globally (Rahman &Singh, 2019). Chromium can be found in food, water, air, and land. It is thought to pose a threat to food security, biodiversity, and the health of the planet (Hasan *et al*., 2019). Plants are severely harmed by chemicals containing chromium, which affects plant development and production. Conversely, certain plants can absorb, relocate, and endure elevated concentrations of Cr, whereas other plants become adversely affected by it. Plants that are exposed to Cr toxicity exhibit a range of symptoms, including decreased yield, altered leaf and root development, reduction of enzyme activity, and mutagenesis (Gill et al., 2014; Shahid et al. 2017).

Numerous conventional remediation techniques have been applied to remove Cr-contaminated soil, sediments, and water. However, these procedures are expensive because they use much energy and chemicals (Shahid et al., 2017). In recent decades, using plants to absorb, collect, and/or break down toxins from contaminated soil, water, sediments, and air has become more prevalent. This process is known as phytoremediation. One of the fastest-evolving aspects of this economical and ecologically friendly technology is the removal of hazardous metals from soil and water by using plants that accumulate metals (Kumar et al., 2018).

The technique of creating particles with at least one dimension between 1 and 100 nm, which produces high surface-to-volume ratios, is called nanotechnology. Nanotechnology in food and pharmaceuticals is developing quickly (Kalashgarani & Babapoor, 2022), in agriculture, water treatment, electronics, cosmetics, and diagnostics. (Gupta et al 2022; Kuhn et al 2022). The diagnostic and therapeutic applications of metallic nanoparticles in various disorders have grown dramatically (Al-Joufi et al, 2022). Nanoparticles demonstrate great results in the discipline of nanotechnology and contribute to addressing the difficulties of the current decade. Pharma and food-related experts use biotechnology with green chemistry to generate breakthrough products that help the environment. An alternative green technique is employed to create nanoparticles rather than chemical ones. The synthesis of AgNPs from the herbal extract is the essential job of green chemistry since the dangerous substances deposited on the surface of nanoparticles during chemical procedures cannot be readily separated and, therefore, impede medicinal use (Hebbalalu et al., 2013). Because of its biocompatibility and electrical properties, Silver is the most effective of the metallic nanoparticles. AgNPs are a class of noble metallic nanoparticles with several uses. Among the metals listed above, AgNPs have sparked much attention due to their unique features for application in pharmaceutics, irrigation, water purification, air filtration, textile industries, and as a catalyst in oxidation processes (Panigrahi, 2013).

Brassicaceae, a mustard family with around 435 genera and 3675 species worldwide, contains the genus Brassica (Mondal & Chakraborty 2020). *Brassica* is a diverse agricultural crop genus with significant global economic value (Salehi *et al*., 2021). *Brassica* species are primarily grown for oil, spices, vegetables, and feed. Brassica species farmed predominantly for trade include rape and mustard seeds (*B. campestris* L., *B. napus* L., and *B. juncea*). (Rai *et al*., 2022). The Brassicaceae family has an outstanding tendency for heavy metal accumulation. (Angelova *et al*., 2017). The Brassicaceae family compensates for the high concentration with

tremendous bioenergy and the ability to collect considerable amounts of HMs. (Yan *et al*., 2020).

MATERIALS AND METHODS

Silver nanoparticles synthesis

A fresh plant (*Dryoptris filix*) was obtained from Bajour, Khyber Pakhtunkhwa, Pakistan, for green production of silver nanoparticles. After that, the plants were thoroughly cleaned under running tap water and then rinsed four times with distilled water to remove any dust particles stuck to the surface. After being fully shade-dried, the collected portion was turned into powder. The powder was moved inside an amber-colored container to prevent contamination and moisture. In order to prepare the extract, four grams of (frond stem and root) were combined with 100 mL of distilled water, dissolved using a stirrer on a hot plate for fifteen minutes at 100 C, and then filtered. The resulting filtrate was employed as an AgNP-reducing agent.

Green synthesis of AgNPs from fronds, stem, and root of *D. filix* was done by Wing et al (2021). Aqueous extract of frond stems and root (250 µg/mL) was combined with 1 mM (0.042g) of AgNO3 aqueous solution and stirred continuously for three hours at room temperature. This process was done to obtain the specific color of silver nanoparticles (dark brown), which were achieved by reducing a silver ion with the aid of phytochemicals representing the AgNPs fabrication process. Physical characterization was used to characterize and synthesize the resulting silver nanoparticles, which were measured by UV spectroscopy of silver nanoparticles solution. (Noruzi *et al*., 2015). The silver nanoparticles were cleaned by spinning at 12000 rpm for 15 minutes and then dried out for further examination.

Ag nanoparticles characterization

Various spectroscopic and microscopic approaches were used to characterize the bio-fabricated Ag NPs. The UV-visible spectrophotometer was used to validate the synthesis and stability of Ag NPs. (Shimadzu UV-1800, Japan). Using a Fourier transform infrared (FTIR) spectrophotometer, several functional groups associated with Ag NPs were found. (Nicolet iS50 FTIR Spectrometer, USA). FTIR analysis was conducted at room temperature using KBr in transmission mode with a frequency range of 400–4000 cm^{-1}. Using X-ray diffraction spectroscopy, the size and crystalline structure of Ag NPs were determined. Using an X-ray diffractometer, diffraction patterns were recorded from the dried Ag NP samples. (Shimadzu-Model XRD 6000). The apparatus was run at 40 kV with a current of 30 mA, scanning 2 in a range of 10-80°. The Debye-Scherrer equation was used to determine the average particle size of the nanoparticles.

$$D = k\lambda/\beta\cos\theta$$

Where D= particle size (nm), k = shape factor (0.94), λ=X-ray wavelength (λ=1.5418 Å), β= full width at half maximum (FWHM), and θ=Bragg's angle.

SEM and TEM microscopy were used to assess the shape and particle size of Ag NPs. (JSM5910 JEOL, Japan) EDS, DSC, AND DTG analysis were used to verify the presence of elemental Ag in AgNPs. The sample was generated by centrifuging a nanoparticle solution at 14,800 rpm for 15 minutes and then drying at 35 _C before being submitted to EDS, DSC, and DTG examination using a thermal instrument attached to an Oxford Inca 200 SEM. (Lab tech., Yokosuka, Japan).

Seed collection

B. campestris L. seeds were obtained from the Department of Agriculture at Abdul Wali Khan University Mardan, Pakistan. Viable seeds were immersed in water for roughly 30 minutes,

then treated with 70% ethanol for surface cleaning for 30 seconds, and rinsed three times with distilled water.

Municipal wastewater collection

Municipal wastewater was collected from sewage water canals near Abdul Wali Khan University Mardan's Garden Campus. The collected wastewater was stored for experimentation in the Plant Ecology Laboratory, Department of Botany, Abdul Wali Khan University Mardan.

Growth media and the addition of chromium

Hoagland's solution was used for the growth medium of the hydroponic culture. Chromium (III) potassium Sulphate ($KCrS_2O_8$) was added to the medium that had been produced according to the usual method at a concentration of 50 mg/L and mixed (Hoagland and Arnon (1950).

Transplanting of seeds

Forceps were used to implant the seeds onto petri plates. Each petri dish contains fifteen (15) healthy seeds, with four copies of each concentration. All plantlets were kept in the growth chamber for one month at 25 ±2 °C with 60-70% relative humidity in light and dark photoperiods. The entire experiment is repeated five times.

Nanoparticles and wastewater treatments

Concentrations After transplanting, plantlets received 50 mg L1 of Ag NPs and wastewater. Sonication for 30 minutes disseminated nanoparticle suspensions in aqueous solutions. (Toshiba, Japan) before adding growth media. To evaluate the effect of Cr stress on plant development, plantlets that had not been exposed to Cr were contrasted with plants that had received Cr treatment. Interventions employed in hydroponic studies: TP (tape water), WW (wastewater), NW (50 mg/L nanoparticles + wastewater), NP (50 mg/L nanoparticles), TPCR (tape water + 50 mg/L chromium), WWCR (wastewater + 50 mg/L chromium), NWCR (50 mg/L nanoparticles + wastewater + 50 mg/L chromium), NPCR (50 mg/L nanoparticles + 50 mg/L chromium).

Plant harvesting and data collection

Thirty days after the treatment was applied, all treated and control plants were duly harvested. Deionized water was then used to clean the roots thoroughly. After measuring the stem and root's length with a centimeter ruler, both were put in a refrigerator to be examined later.

Physico-chemical characterization

The T.D.S of wastewater was measured by a portable meter (HI991300 portable waterproof PH/EC/TDS Meter). Dissolved Oxygen in wastewater administered by a Portable Multi-Parameter Meter (9000P). The dissolved oxygen (DO) quantity was measured with the Portable Multi-Parameter Meter. (9000P). The BOD_5 technique was used to calculate the biochemical oxygen demand (BOD). On day one, the first DO measurement was taken, and five days were spent with the water samples in an incubator at 20 °C. On the sixth day, another reading of the DO was taken. (Nizam et al., 2020).

The formula for calculating BOD5 is as follows:

BOD5 = DO (reading on the first day) – DO (reading on the fifth day)

Measurements of Turbidity were performed by a Turbidity meter (SPER SCIENTIFIC Turbidity Meter 860040). PH was measured by a portable pH meter. The ORP level in wastewater was measured by a Portable Multi-Parameter Meter (9000P). COD and Multi-Parameter Photometer measured the Ammonia, Cyanide, Aluminum, Copper, Chromium,

Nickel, Zinc, Iron, Bromine, Alkalinity, Free Chlorine, Color of Water, Nitrate, Magnesium Hardness and Magnesium. (APHA-3111) & (Multi-Parameter Photometer HI8309).

Photosynthetic pigments

B. campestris L. leaves' chlorophylls (a & b), and carotenoid content were calculated using the method described by Sumanta et al. (2014). After completely homogenizing fresh leaves (0.5 g) in 10 mL of 80% acetone, the leaves were spun in a centrifuge for 15 minutes at 10,000 rpm. Supernatants were separated using 4.5 mL of 80% acetone in sterile test tubes. Using a spectrophotometer, the absorbance of the samples was measured at 645, 663, 510, and 470 nm.

Phenol and flavonoids

Total flavonoid content (TFC) in plant samples was estimated using the aluminum chloride technique (El Far & Taie, 2009). In summary, 500 µL of the plant extract or supernatant was combined with 4.8 mL of 80% methanol, 100µL of 10% potassium acetate, and 100µL of aluminum chloride. After providing the mixture with an adequate shake, it was incubated for 30 minutes. After incubation, optical density was measured at 415 nm. The Folin-Ciocalteu technique was used to assess the phenolic contents of the plant samples (Prabhavathi et al., 2016). In summary, 800µL of Folin-Ciocalteu reagent and 2 mL of 7.5% sodium carbonate were added to 200µL of the sample extract. After diluting the entire fluid to seven volumes with distilled water, it was incubated for two hours. Different amounts of catechol were handled as described above for the standard curve, and optical density was measured at 765 nm versus blank.

Protein estimation

The protein content of the leaves was measured using the Niiforovi et al. (2010) methodology. 100 mg of leaves were homogenized in a phosphate buffer (1 mL, pH 7.5) and centrifuged at 10,000 rpm for 15 minutes to extract protein. The distilled water was used to dilute the extract (100 L) to form a 1 mL solution. 1 mL of copper reagent (2% sodium carbonate, 0.1 N sodium hydroxide, 1% Copper Sulphate, and 2% sodium potassium tartrate) was added to the diluted extract and well mixed for 10 minutes. The mixture was incubated in an incubator at room temperature for 30 minutes with diluted Folin-Ciocalteau reagent (100 L). A spectrophotometer was used to measure absorbance at 650 nm.

Estimation of soluble Sugar

Brassica campestris L. was found to have soluble sugars utilizing the Mohammadkhani and Heidari (2008) approach. A 0.5 g fresh leaf weight was homogenized with DW, and the resulting extract was filtered before being treated with 98% sulfuric acid and 5% phenol. After allowing the mixture to settle for an hour, the absorbance at 485 nm was measured with a spectrophotometer. Benedict's response serves as a starting point. The amount of soluble sugar was provided in milligrams g-1 FW.

Antioxidant activity determination

The antioxidant capacity of different *Brassica campestris* L. sections was evaluated using the Ahmad et al. (2010) method and DPPH, a stable free radical. 1 diphenyl-2-picrylhydrazyl. The absorbance of different reaction solutions at 517 nm was measured using UV-visible spectroscopy (Shimadzu, Japan). The antioxidant activity was calculated as a percentage of the DPPH solution's discoloration using the following equation: Free radical scavenging action of DPPH (%) = $[A_c\text{-}A_s/A_c]$ 100, where (AS) represents sample absorbance and (AC) represents DPPH solution absorbance.

Determination of enzymatic activities

The initial H_2O_2 cleavage rate was used to calculate CAT activity (Radhakrishnan & Lee, 2013). Cool mortar and pestle were used to smash fresh leaves (0.5 g). After that, the ground material was homogenized in 10 mL of 50 mM phosphate buffer (pH 7.0) containing 1 mL Na2-EDTA and 2% (w/v) polyvinylpyrrolidine-40 (PVP-40). After that, the mixture was centrifuged at 11000 g for 15 minutes at 4 °C. In 0.05 M Na-phosphate buffer (pH 7), 0.1 mL of supernatant sample was mixed with 3% (v/v) H_2O_2 and 0.1 mM EDTA. The drop in H_2O_2 causes a decrease in O.D at 240 nm, which was depicted as a breakdown of M H2O2 min 1. Lagrimini (1991) technique was used to determine peroxidase activity. To homogenize 0.3 grams of fresh leaf tissue, a phosphate buffer with a pH of 6.8 was utilized. The supernatant was collected after centrifuging the combined extract for 13 minutes at 4 °C and 13500 rpm. The activity of enzymes was tested in the clear supernatant. Phosphate buffer at pH 6.8 (0.1 M). 50 L Pyrogallol, 50 L H_2O_2, and 0.1 mL enzyme extract were utilized. The reaction was halted after 5 minutes of incubation at 25°C by adding 0.5 ml of 5% H_2SO_4 to the liquid. The absorbance at 420 nm was measured using a spectrophotometer.

Chromium analysis

Chromium concentrations were measured in dried ground plant samples. Approximately 0.5 g of finely powdered pulverized dried plant components were placed in digestion vials. Each sample received 6.5 mL of acid solution (HNO_3, H_2SO_4, $HClO_4$) in a 5:1:0.5 ratio for digestion. After soaking for 12 hours, the samples were torched at 300 °C for 3 hours until white vapors appeared. Distilled water was added to the sample to dilute it before filtering it using Whatman filter paper No. 1. An atomic absorption spectrophotometer was then used to determine the ionic content. (AAS 4000) (Aziz et al., 2021).

RESULTS AND DISCUSSION

Characterization of Ag nanoparticles

The green *Dryopteris filix* AgNPs synthesized were examined using PerkinElmer Spectrum UV-Spectroscopy. To evaluate the absorbance of greenly synthesized AgNPs, a variety of reaction mixtures, including 1 mM Ag aqueous solution and plant aqueous extract, were generated, including 1:1, 1:2, 1:3, 1:4, 1:5, and 1:6. As the reaction continued, the hue of the solution changed from pale to dark brown, indicating that AgNPs were produced. In the reaction mixture, several peaks could be detected, whereas, in Fig. 1 (A), the green absorbance peaks of the synthesized silver nanoparticles (AgNPs) occurred in sample 1:5 Mm at 450 nm. Similar findings have been reported for callus-mediated silver nanoparticle production (Anjum & Abbasi 2016).

FTIR analysis

The FT-IR spectra of *Dryopteris filix* aqueous extract show numerous bands at 3319, 2919, 2848, 1634, 2968, 842, and 504 cm-1 capping of AgNPs. The presence of bands at 3319 and 1634 cm-1 might be explained by the continual stretching of the (O- H) and C=O groups. Minor bands at 2929 and 2848 cm1 may be caused by the stretching of alkanes (C- H). The crisp, powerful band detected at 1634 cm1 might be caused by the stretching vibration of the alkene C=C group. Fig 1 (C), the band at locations 2968, 2919, and 1634 on the recorded spectrum is caused by C-O stretching vibration. The AgNPs band was discovered around 450-504 cm, and the discovery was validated by (Acay *et al*., 2019). Little bands in the 842-504 cm1 area might indicate C-C stretching. The AgNPs band was discovered between 450 and 504 cm1. Because of the utilization of *Syzygium cumini* plant extracts, the current finding is compatible with (Chakravarty et al., 2022).

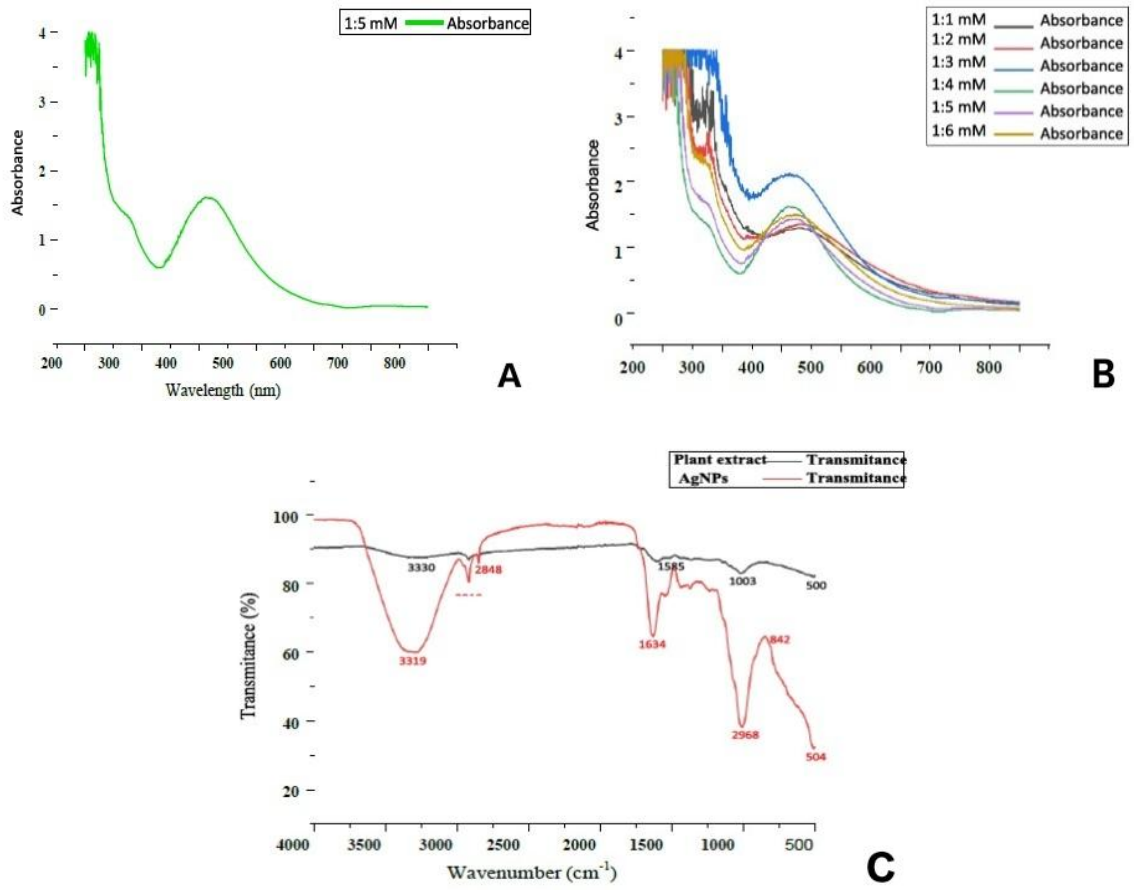

Fig. 1 Show (A) UV-Spectroscopic analyses (B) Different UV-Spectroscopy absorbance peaks (C) FTIR analysis of synthesized AgNPs of *Dryopteris filix* fronds, stem,and root extract

TEM and SEM

In the 20–80 nm size range, the spherical NPs were easily seen and dispersed. When spherical polydispersed AgNPs are produced, they are spherical in form and polydispersed with a range of sizes, as may be seen under a scanning electron microscope. The SEM analysis of silver nanoparticles using *Euphorbia hirta* leaf extract by Devi et al. (2014) revealed that the particles have a spherical and cubic shape. Thombre et al. (2013) state that SEM studies confirmed the presence of roughly spherical silver nanoparticles.

Using transmission electron microscopy (TEM), we can additionally look at the nanoparticles' size, shape, and distribution. For TEM investigation, these nanoparticles were suspended on a copper grid coated with carbon. The average size of the spherically shaped particles is around 14 nm. The interaction between the biomolecules in the extract is responsible for the production of spherical nanoparticles (NPs). According to Mofolo et al. (2020), the NPs' spherical and opaque appearance at different grid points showed that they are uniformly sized and stable at 100 nm, with no obvious agglomeration or aggregation.

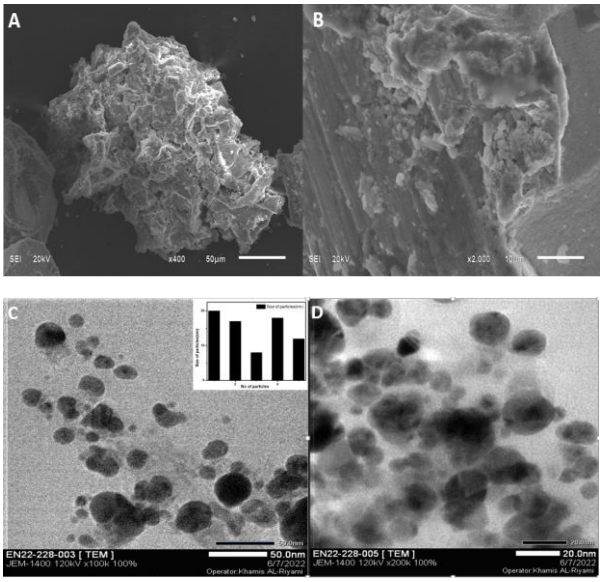

Fig. 2 SEM (A, B) and TEM(C, D) images (insight shows histogram) of silver nanoparticles.

EDX, DSC, and DTG

The primary component of the EDAX spectrum is Ag. The elemental distribution diagram (EDS) indicated the presence of silver (Ag), oxygen (O), and chlorine (Cl) in the sample. The presence of elemental Ag was indicated by the presence of 3 keV peaks. The extract's undefined peaks are biomolecules that have not been processed. Using EDX spectroscopy, the fundamental composition of the silver nanoparticles prepared by Mofolo et al. (2020) from *Pechuel-loeschea leubnitzia* was investigated. Their results confirmed the presence of carbon, nitrogen, oxygen, and the metal silver. Thermo-gravimetric analysis-differential Scanning Calorimetry (DSC) and derivative. The thermal behavior of the silver nanoparticles was examined using thermogravimetry (DTG). The thermal stability and purity of AgNPs were assessed simultaneously using DSC-TGA analysis, as shown in Fig 3 (B). The achieved melting point of 973.22 °C, which was closely matched to the stated metallic silver temperature of 960.54 °C, indicates the purity of the synthesized AgNPs. The initial step of the breakdown process, which happened between 100 and 120 °C, could have been caused by the evaporation of moisture that had been adsorbed on the AgNPs' surface. An additional 19% of body weight was lost, along with a worsening between 400 and 480 °C. The deterioration seen in the silver nanoparticles was probably due to the heat breakdown of resistant aromatic compounds. The bioactive organic compounds from the extract were clearly bonded to the surface of the generated nanoparticles, as demonstrated by the TGA data. The percentage of organic shell was found to be 30%, which is in line with findings from other studies. Elemike *et al*., (2017) discovered that the presence of both endothermic and exothermic activity is correlated with the DSC curve. The DTG plot of PF@AgNPs showed three notable weight losses of 0.14, 0.24, and 0.18% at 111.25, 180.75, and 328.75°C, respectively (Reddy *et al*., 2021). TGA experiments indicate that biosynthesized Ag NPs may be used at temperatures up to 200 °C (Elmusa *et al*., 2021).

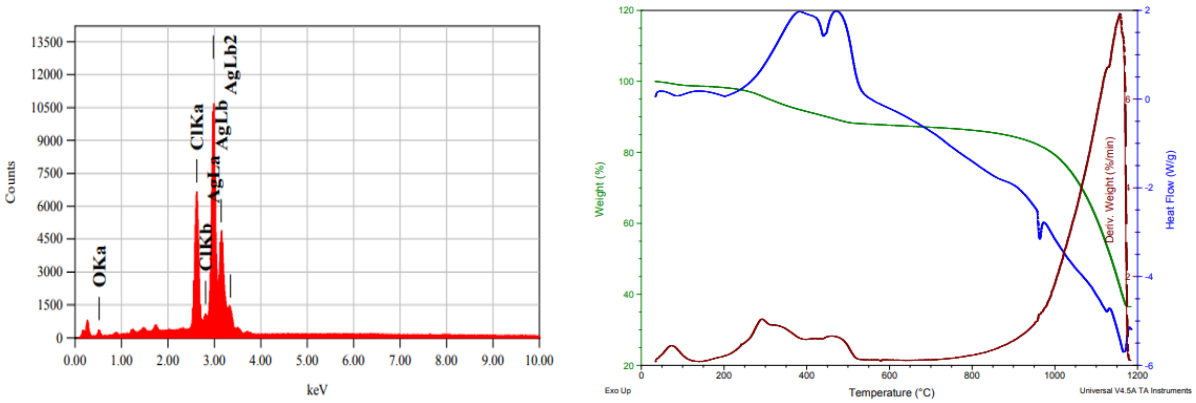

Fig. 3 (A) EDX images and (B) TGA/DSC/DTG graphs of silver nanoparticles.

Physio-Chemical Parameters

The table 1 shows the results of different parameters of wastewater with (NEQS) National environmental quality standard limits.

Table 1. Physio-chemical parameters of wastewater.

S. No	Parameters	Analysis method	Unit	LOR	Result	NEQS
1	pH	pH Meter	-	0.01	4.97	6.5-8.5
2	Dissolved oxygen	SPER scientific	mg/L	-	11.39	Non-Objectionable
3	Biological oxygen demand	SPER scientific	mg/L	1.0	8.1	80
4	ORP	SPER scientific	Mv	-	5.2	Non-Objectionable
5	Turbidity	SPER scientific 460040	NTU	-	7.46	<5 NTU
6	Total Dissolved Solid	APHA-2540	mg/L	1.0	1549	< 1000
7	Cyanide	Multi-Parameter Photometer HI8309	mg/L	0.01	5	≤ 0.05
8	Aluminum	APHA-3111 AI B	mg/L	0.028	0.25	≤ 0.2
9	Copper	APHA-3111 CU B	mg/L	0.0045	0.46	2
10	Chromium	APHA-3111 Cr B	mg/L	0.0054	0.04	≤ 0.05 (P)
11	Nickel	APHA-3111 Ni B	mg/L	0.008	0.31	≤ 0.02
12	Zinc	APHA 3111 Zn B	mg/L	0.0033	0.12	5.0
13	Alkalinity	Multi-Parameter Photometer HI8309	mg/L	-	20	<500
14	Bromine	APHA-3111 Br B	mg/L	0.1	1.09	<50
15	Color of water		PCU	1.0	126	<15TCU

		Multi-Parameter Photometer HI8309				
16	Free chlorine	Multi-Parameter Photometer HI8309	mg/L	0.1	0.12	0.2-0.5
17	Nitrate	Multi-Parameter Photometer HI8309	mg/L	0.1	5.9	<50
18	Magnesium	Multi-Parameter Photometer HI8309	mg/L	-	65	<250
19	Magnesium hardness	Photometer HI8309	mg/L		0.42	<250

ND: Not Detected **LOR:** Limit of Reporting, **BDL:** Below Detection Limit, **NEQS:** National Environmental Quality Standard

Seedling Growth

Brassica campestris L. seeds were grown in petri dishes. For this experiment, eight sets of seedlings were grown for 25 to 30 days. The first set was controlled without stress treatment, which included tap water, wastewater, and nanoparticles at 50 mg/L while another set was treated with chromium stress at 50 mg/L. Chromium was added to the plant with adjoining nanoparticles, tap water, and Wastewater. The plants were harvested, their shoot and root lengths were measured, and their fresh and dry weights were calculated. The biochemical analysis of several treatment groups of *Brassica campestris* L. was evaluated with the use of a spectrophotometer.

Root Shoot length and Fresh Dry weight

The Nanoparticles (NP) promote root and shoot length in *Brassica campestris* L. as compared to TP, WW, and NW. Seedlings with nanoparticles (NP) showed growth promotion and improved root and shoot length (15.1 cm & 6.95 cm), and wastewater (WW) showed a reduction in root and shoot length (13 cm & 4.05 cm) without chromium stress condition. The current findings are consistent with the findings of (Sharma *et al*., 2012), who discovered that silver nanoparticle treatment increased the development of *B. juncea* seedlings by 25 and 50 ppm. While in stress condition, NWCR and NPCR showed the best results of SL (4.20 and 4.80 cm) as compared to TPCR (3.75 cm) and WWCR (3.7 cm). (Fig. 4 a & b). According to Death (Becerra-Castro *et al*., 2015), the application of industrial effluent containing high concentrations of metals such as Pb, Cr, Cd, Cu, Fe, Zn, and Ni decreases plant development by limiting photosynthesis, inducing senescence, and affecting nutrient absorption and water balance, culminating in plant mortality.

The plant associated with nanoparticles resulted in a significant increase in fresh and dry weight. The seedling associated with NP had a higher fresh weight (62 mg) and dry weight (20.6 mg), while a lower weight showed in TP and WW respectively. (Fig 4 c & d). The NW showed high results from TP and WW and lower results from NP without stress conditions. The treatment group that used AgNPs-40 in addition to wastewater demonstrated a beneficial impact on root/shoot fresh and dry weights in *C. annuum* (Aqeel *et al*., 2023). In applying 50 mg/L chromium stress to the seedlings, NWCR (FW 43.5 mg, DW 14.5 mg) and NPCR (FW 45.5 mg, DW 15.4 mg) show higher results as compared to TPCR and WWCR, respectively (Fig. 4.8 C) Our findings are consistent with those made by (Shahid *et al*., 2015) and (El-Shahir *et al*., 2021) who found that exposure to heavy metals significantly reduced plant height, root length, and the fresh and dry weights of shoots and roots.

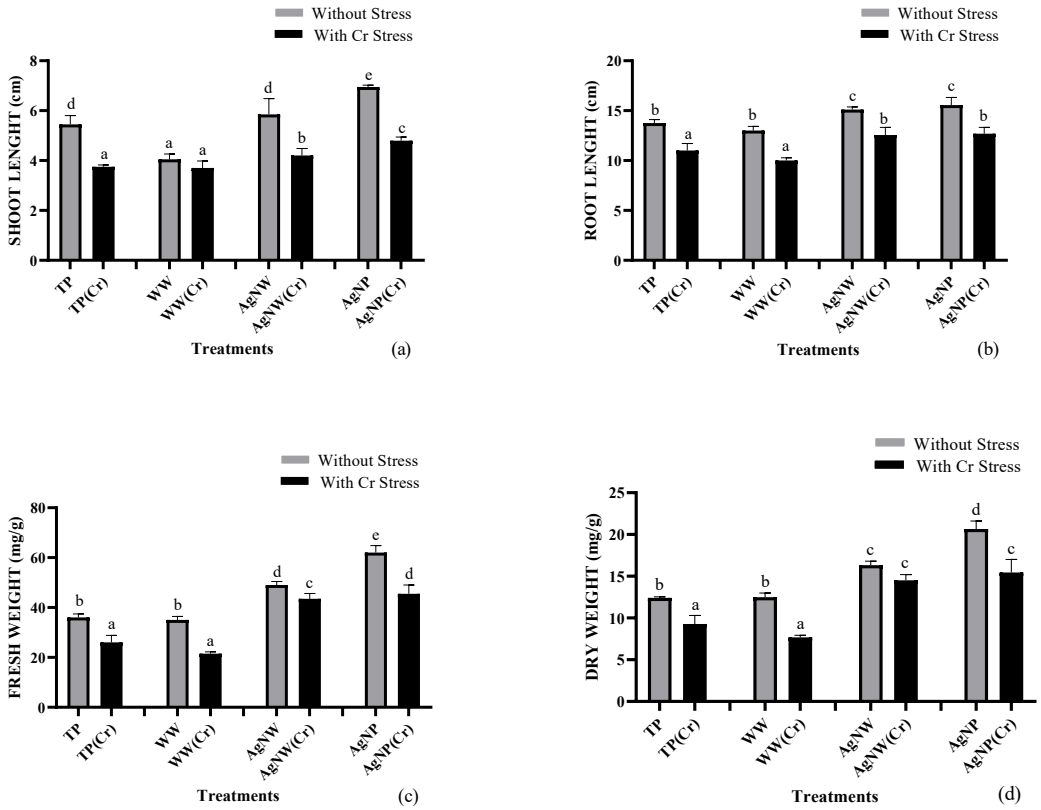

Fig. 4 Measurement of A) Shoot Length, B. Root Length, C. Fresh Weight D. Dry Weight of *Brassica campestris* L. under Chromium stress and without stress condition. Each bar represents the tripled data's mean along with its standard error. The different bars' letter labels on the graphs show which differences are significant at $p < 0.05$.

Photosynthetic pigments

The silver nanoparticles 50 mg/L meaningfully increase chlorophyll a (1.58 mg/g), and chlorophyll b (1.24 mg/g) contents in *B. campestris* L. The chlorophyll a (1.17 mg/g), and chlorophyll b (0.95 mg/g) in WW show reduction. The TP (chl a 1.47 mg/g & chl b 1.20mg/g) and NW (chl a 1.52 mg/g & chl b 1.10 mg/g) show results in between them in absence of chromium stress while to give 50 mg/L chromium stress to seedling the NPCR (chl a 1.02 mg/g & chl b 0.83 mg/g) shows a higher result than TPCR (chl a 0.85 mg/g & chl b 0.74 mg/g),WWCR (chl a 0.82 mg/g & chl b 0.63 mg/g) and NWCR (chl a 0.96 mg/g & chl b 0.78 mg/g) respectively. (Fig 5 a & b). An increase in chlorophyll contents was seen at silver nanoparticle treatment concentrations of 25, 50, and 100 ppm. The greatest increases in chlorophyll-a and total chlorophyll content were found to be 40% and 25%, respectively, at 100 ppm silver nanoparticle treatment (Sharma *et al*., 2012). When wheat seedlings received irrigation with sewage water, (Liu *et al*., 2002) noted a decrease in the chlorophyll content. In response to wastewater irrigation, the seedlings' leaves had less chlorophyll a and b. Seedlings associated with nanoparticles NP showed higher total chlorophyll content in plants while wastewater WW showed lower content without stress. In Cr stress conditions, NWCR and NPCR showed higher results in *Brassica campestris* L. as compared to TPCR and WWCR. (Fig 5 c). The graph clearly shows that adding nanoparticles to plants substantially improved the amount of carotenoids. In the absence of chromium, the highest levels of carotenoids were found in TP (0.72 mg/g) and NP (0.73 mg/g) while in addition to chromium stress, TPCR (0.375 mg/g) and WWCR

(0.29 mg/g) had reduced carotenoids contents as compared to NWCR (0.53 mg/g) and NPCR (0.53 mg/g). (Fig 5 d). Higher concentrations of heavy metals may be linked to wastewater-induced reductions in chlorophyll content (Gadallah 1995). According to (Monnie *et al*., 2001 and Patsikka *et al*., 2002). The amount of chlorophyll is higher in control veggies; this might be because stress causes chlorophyll to break down or because chlorophyll production is suppressed. Metal toxicity has been linked to lower chlorophyll levels in vascular plants. Heavy metal poisoning caused a considerable reduction in chlorophyll a, chlorophyll b, and carotenoid concentrations in carrot plant leaves in this research (Batal *et al*., 2023). Chromium stress negatively affects the shoot and root length of *Brassica campestris* L., while nanoparticles alleviate the negative effect on the shoot length under the influence of chromium stress.

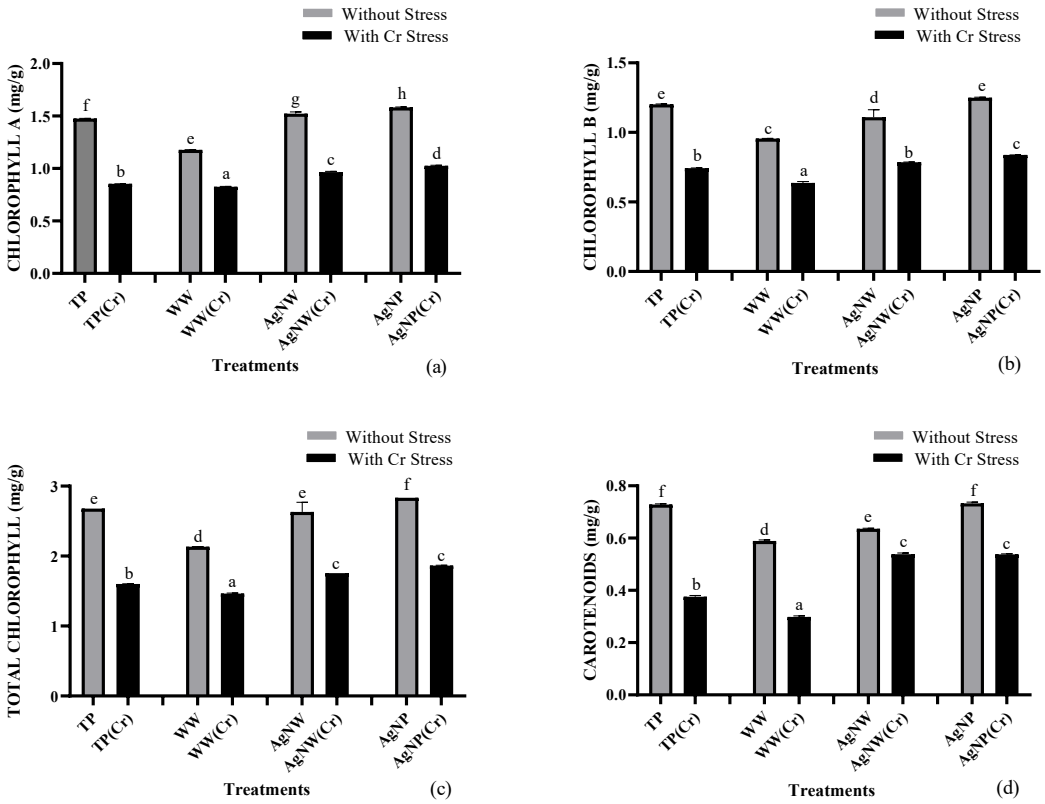

Fig. 5 Photosynthetic pigments A) Chlorophyll a, B) Chlorophyll b, C) Total chlorophyll, D) Carotenoids in *Brassica campestris* L. plant under chromium stress and without stress condition. Each bar represents the tripled data's mean along with its standard error. The different bars' letter labels on the graphs show which differences are significant at $p < 0.05$.

Phenol and flavonoid contents

The phenol amount of *Brassica campestris* L. was measured under stress and control conditions. Without chromium stress, the phenol contents of *Brassica campestris* L. with TP (14.6 mg/g), WW (14.38 mg/g), NW (15.92 mg/g), and NP (16.69 mg/g) showed longer growth as compared to stress condition. However, under chromium stress, the phenol contents were generally reduced, as seen with TPCR (6.74mg/g), WWCR (6.24 mg/g), NWCR (9.93 mg/g), and NPCR (12.84 mg/g) (Fig 6 a). ZnO NPs enhanced total phenolics at all concentrations examined (Hussain *et al*., 2021. The NP and NPCR showed higher contents in stress and without stress conditions. Chromium stress reduces the phenol content of *Brassica campestris* L., whereas nanoparticles mitigate this effect.

The plant treated with nanoparticles produced a noticeable rise in the amount of flavonoids. The seedling associated with NP had higher contents (1.92 mg/g) while lower contents showed in WW (0.88 mg/g). The NW (1.75 mg/g) showed high results from TP and WW and lower from NP without stress condition (Fig 6 b). In applying chromium stress to the seedlings the WWCR shows lower results (0.60 mg/g) as compared to TPCR (1.53 mg/g) and NWCR (1.67 mg/g). Higher results shown in NPCR (1.84 mg/g) respectively. These findings are consistent with those of (Zafar *et al*., 2016), who reported a dose-dependent increase in flavonoids with ZnO NPs in *B. nigra* seedlings. However, the phenolic content of plants grown only on sewage sludge was reduced (Burducea *et al*., 2019). (Batal *et al*, 2023) reported that phenol levels in heavy metal-stressed carrot plants were considerably raised by selenium nanoparticles.

Total sugar and protein contents

The current result of protein content illustrates that the application of chromium stress shows a significant reduction as compared to without stress (Fig 6 c). The NW, NP, NWCR, and NPCR showed higher results in stress and without-stress conditions while reduction was recorded in TP, TPCR, WW, and WWCR. The values noted under stress and without stress conditions are TP (91.3 mg/g), TPCR is (48.1 mg/g), WW (90.7 mg/g), WWCR (44.9 mg/g), NW (92.0 mg/g), NWCR (50.3 mg/g), AgNP (94.04 mg/g) and NPCR (53.5 mg/g).

The sugar contents in B. campestris L. is increased in NP (1.38 mg//g) concentration in the control set. The contents are reduced in WW (1.06 mg/g) meaningfully. The NW (1.36 mg/g) and TP (1.08 mg/g) result show that they while adding chromium to these concentrations the NPCR (1.01 mg/g) shows higher results against stress compared to other concentrations. (Fig 6 d). The current result was supported by (Sadak 2019) comparing fenugreek plants treated with foliar AgNP to control plants, total carbohydrates and protein increased significantly; the greatest levels of these increases were again attained at 40 mg/l AgNPs. (Rong Guo *et al*. 2007, Hsu, and Kao 2003) reported that in the samples from wastewater-irrigated plants, the leaf portion of *R. sativus* and *B. nigra* has decreased protein content. Further (Oyiga *et al*., 2016) examined that carbohydrate reduction as a result of wastewater might be related to nitrogen imbalance and decreased photosynthesis. Because high levels of Na+ in the leaves of wastewater-irrigated plants decrease the delivery of carbohydrates to immature leaves, high levels of Na+ can explain the lower leaf area. Stress causes a decrease in soluble protein content in plants while increasing soluble sugar content (Rong Guo *et al*. 2007 & Hsu and Kao 2003). In *Brassica campestris* L. sugar and protein contents are significantly impacted by chromium stress, while the detrimental impact has been mitigated by the use of nanoparticles.

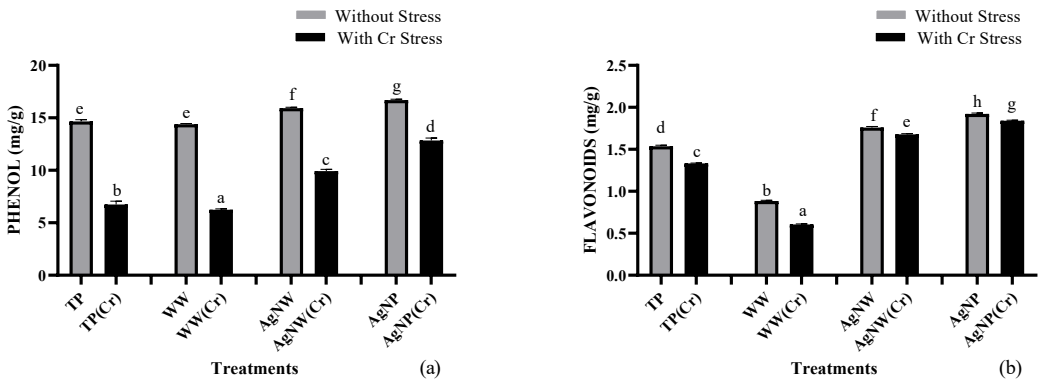

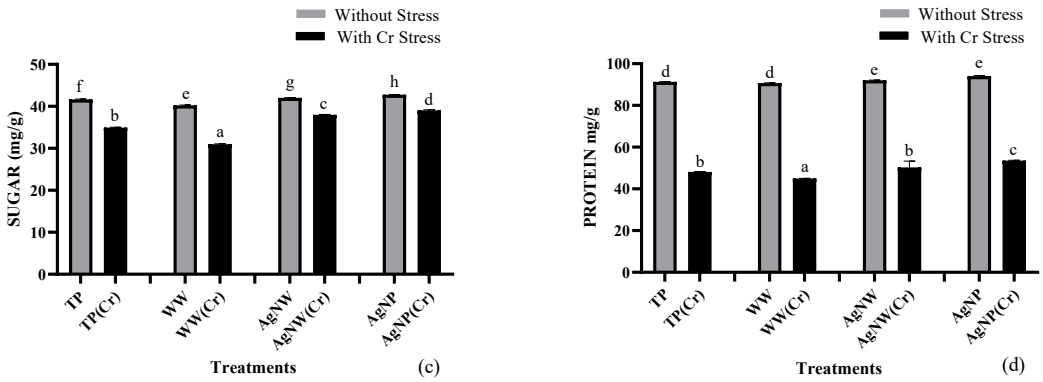

Fig. 6 Quantification of A) Phenol, B) Flavonoids C) Sugar, D) Protein in *Brassica campestris* L. plant under chromium stress and without stress condition. Each bar represents the tripled data's mean along with its standard error. The different bars' letter labels on the graphs show which differences are significant at $p < 0.05$.

IAA

The current result of indole acetic acid content illustrates that the application of chromium stress shows a significant reduction as compared to the absence of stress. The NP showed higher contents in the absence of chromium although in the presence of chromium, NPCR also showed higher contents while reduction is recorded in WW and WWCR (Fig 7 a). The values noted under stress and without stress conditions are tap water TP (1.08 mg/g), TPCR is (0.97 mg/g), WW (1.06 mg/g), WWCR (0.93 mg/g), NW (1.36 mg/g), NWCR (0.99 mg/g), NP (1.38 mg/g), NPCR (1.01 mg/g). The current results were supported by (Sadak 2019). Spraying fenugreek plants with different amounts of AgNPs significantly raised IAA, with 40mg/l of AgNPs resulting in the greatest level of IAA compared to the comparable control plants. When compared to wastewater, silver nanoparticles dramatically increased the IAA, GA, and ABA concentrations (Khan and Bano 2016).

Antioxidant Activity

Using the DPPH free radical scavenging assessment, antioxidant capacity in various plant tissues under stress and without stress treatments can be seen in (Fig 7 b). Based on the most recent results, antioxidant activity in plant tissues was increased in WWCR (1.4 mg/g) during chromium stress in comparison with TPCR (1.29 mg/g), NWCR (1.09 mg/g), and NPCR (1.09 mg/g), as well as in increased WW in a stress-free condition in compared to TP, NW, and NP. Similarly DPPH antioxidant capacity of *Gynura procumbens* (Lour.) Merr. was significantly increased in plants treated with copper and cadmium (Ibrahim et al. 2017).

CAT and POD

The Fig. 7 c demonstrates the influence of nanoparticle, chromium, and wastewater treatments on peroxidase (POD) activity in *B. campestris* L. leaves. In the current research, relative to TPCR, NWCR, and NPCR, Chromium stress WWCR substantially boosted peroxidase activity in leaves of *B. campestris* L. while in the absence of Chromium, the WW significantly increased. These results indicated that the maximum peroxidase activity in leaves was produced by wastewater and chromium at moderate concentrations of WW and WWCR (0.104 units/g FW & 0.219 units/g FW). However, the POD activity of *B. campestris* L. plant leaves was decreased by the NW, NP, NWCR, and NPCR concentrations. According to (Batal *et al*., 2023) if carrot plants were watered with wastewater, their peroxidase (POD) and catalase (CAT) activity were much higher than in unirrigated plants. Peroxidases are important in the defense against oxidative stress and have been proposed as markers of metal toxicity (Radotic *et al*.,

2000). Increased peroxidase activity has also been seen in palak (Beta vulgaris var All green) cultivated at various sewage sludge application rates (Singh and Agrawal, 2007).

The total catalase activity of *Brassica campestris* L. seedling treated with nanoparticle wastewater and chromium was determined through a spectrophotometer. In this current study, Chromium stress WWCR considerably increased catalase activity in *B. campestris* L. leaves in comparison with TPCR, NWCR, and NPCR, although in the absence of Cr stress, WW substantially increased. These results indicated that wastewater and chromium at a moderate level of WWCR and WW generated the most effective catalase activity in leaves (Fig 7 d). However, the concentrations of NW, NP, NWCR, and NPCR decreased the catalase activity of *B. campestris* L. leaves. Catalase is in responsible for degrading the accumulated hydrogen peroxide (Dixit *et al*., 2001). The rise in catalase activity in *T. latifolia* following heavy metal exposure implies that the HM-induced breakdown of hydrogen peroxide is operating. Catalase activity was increased in all heavy metal-treated *T. latifolia* leaves, supporting this idea. (Schröder and Lyubenova 2011).

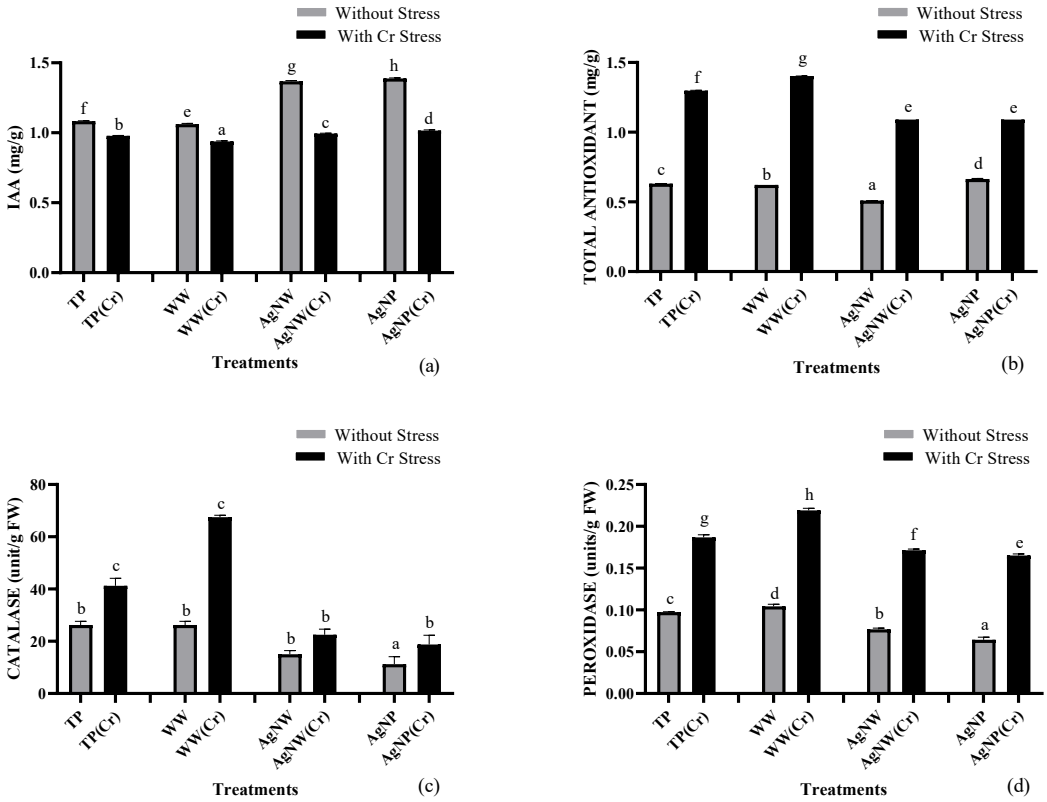

Fig. 7 Quantification of A) IAA, B) Antioxidant Activity, C) Peroxidase, D) Catalase in *Brassica campestris* L. plant under chromium stress and without stress condition. Each bar represents the tripled data's mean along with its standard error. The different bars' letter labels on the graphs show which differences are significant at $p < 0.05$.

Chromium accumulation, bio concentration and translocation

The concentrations of Cr in the roots and shoots of *Brassica campestris* L. after treatment with tap water, wastewater, and nanoparticles are demonstrated in the corresponding figures. The Cr concentration in root and shoot was significantly increased with WWCR (131.4 and 82.2 mg/kg). Maximum Cr content in roots and shoots (117.8 & 72.62 mg/kg) and (104.6 & 60.8)

respectively were found in NWCR and NPCR. The TPCR showed root and shoot levels is (123 and 77.8 mg/kg). Moreover, the level of NPs (50 mg L−1) decreased Cr concentration in different tissues. The present work corresponds to (Alharby and Ali 2022) Fe NPs and *S. aureus* L. applied together considerably decreased the absorption and accumulation of Cr in the plants. According to (Singh and Agrawal 2007) Cd had the greatest increase in heavy metal absorption in plants as a result of sewage sludge amendment, followed by Ni, Pb, Cr, Cu, and Zn. Metal or metal oxide nanoparticles are utilized in wastewater treatment to remove heavy metal ions (Khan and Bano 2016).

The bioconcentration factor value from root to shoot shows in WWCR is higher than other concentrations. The lowest factor is shown in NPCR while TPCR and NWCR is between of them.

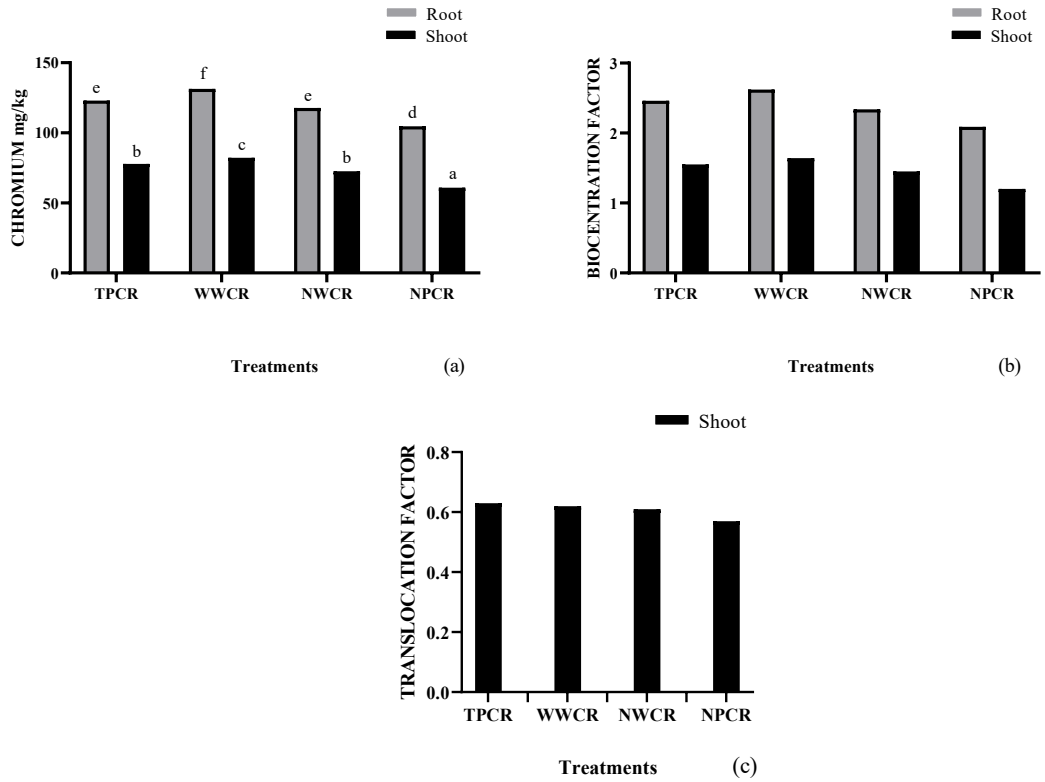

Fig. 8 (A) Uptake (B) Bioconcentration (C) Translocation of Chromium in Root to shoot of *Brassica campestris* L.

References:

Acay, h. and baran, m.f., 2019. Investigating antimicrobial activity of silver nanoparticles produceed through green syn thesis using leaf extract of common grape (*vitis vinifera*.

AhmadN, Fazal H, Abbasi BH, RashidM,Mahmood T, Fatima N (2010) Efficient regeneration and antioxidant potential in regenerated tissues of Piper nigrum L. Plant Cell Tissue Organ Cult 102:129–134

Alharby, H.F. and Ali, S., 2022. Combined role of Fe nanoparticles (Fe NPs) and Staphylococcus aureus L. in the alleviation of chromium stress in rice plants. *Life*, *12*(3), p.338.

Al-Joufi, F.A.; Setia, A.; Salem-Bekhit, M.M.; Sahu, R.K.; Alqahtani, F.Y.; Widyowati, R.; Aleanizy, F.S. Molecular pathogenesis of colorectal cancer with an emphasis on recent advances in biomarkers, as well as nanotechnology-based diagnostic and therapeutic approaches. *Nanomaterials* **2022**, 12, 169. [CrossRef] [PubMed]

Anjum S, Abbasi BH (2016) Thidiazuron-enhanced biosynthesis and antimicrobial efficacy of silver nanoparticles via improving phytochemical reducing potential in callus culture of *Linum usitatissimum* L. Int J Nanomedicine 11:715–728

Aqeel, M., Khalid, N., Nazir, A., Irshad, M.K., Hakami, O., Basahi, M.A., Alamri, S., Hashem, M. and Noman, A., 2023. Foliar application of silver nanoparticles mitigated nutritional and biochemical perturbations in chilli pepper fertigated with domestic wastewater. *Plant Physiology and Biochemistry*, *194*, pp.470-479.

Aziz, L., Hamayun, M., Rauf, M., Iqbal, A., Arif, M., Husssin Khan, A. S.A., et al (2021). Endophytic Aspergillus Niger Reprograms the Physicochemical Traits of Tomato Under Cadmium and Chromium Stress. Environmental a n d Ex p e r i m e n t a l Bo t a n y , 1 8 6 , 1 0 4 4 5 6 . d o i : 1 0 . 1 0 1 6 / j.envexpbot.2021.104456

Batal, M., Deaconu, A. and Steinhouse, L., 2023. The nutrition transition and the double burden of malnutrition. In *Nutritional Health: Strategies for Disease Prevention* (pp. 33-44). Cham: Springer International Publishing.

Becerra-Castro, C., Lopes, A. R., Vaz-Moreira, I., Silva, E. F., Manaia, C. M., & Nunes, O. C. (2015). Wastewater reuse in irrigation: A microbiological perspective on evaluation software (SIDES). *Computers and Electronics in Agriculture, 100*, 100–109.

Briffa, J., Sinagra, E. and Blundell, R., 2020. Heavy metal pollution in the environment and their toxicological effects on humans. *Heliyon*, *6*(9).

Burducea, M., Lobiuc, A., Asandulesa, M., Zaltariov, M.F., Burducea, I., Popescu, S.M. and Zheljazkov, V.D., 2019. Effects of sewage sludge amendments on the growth and physiology of sweet basil. *Agronomy*, *9*(9), p.548.

Chakravarty, A., Ahmad, I., Singh, P., Sheikh, M.U.D., Aalam, G., Sagad, Evan, S., and Ikram, S., 2022. Green synthesis of silver nanoparticles using fruits extracts of Syzygium cuminiand their Bioactivity. Chemical Physics Letters, p.139493.

Chen, M., Xu, P., Zeng, G., Yang, C., Huang, D., Zhang, J., 2015. Bioremediation of soils contaminated with polycyclic aromatic hydrocarbons, petroleum, pesticides, chlorophenols and heavy metals by composting: applications, microbes and future research needs. Biotechnol. Adv. 33, 745e755.

Devi, G.D., Murugan, K. and Selvam, C.P., 2014. Green synthesis of silver nanoparticles using Euphorbia hirta (Euphorbiaceae) leaf extract against crop pest of cotton bollworm, Helicoverpa armigera (Lepidoptera: Noctuidae). *Journal of Biopesticides*, *7*, p.54.

Dhanarani, S., Viswanathan, E., Piruthiviraj, P., Arivalagan, P., Kaliannan, T., 2016. Comparative study on the biosorption of aluminum by free and immobilized cells of *Bacillus safensis* KTSMBNL 26 isolated from explosive contaminated soil. J. Taiwan Inst. Chem. Eng. 69, 61e67.

Dixit, V., Pandey, R., Shyam, R., 2001. Differential antioxidative responses to cadmium in roots and leaves of pea (Pisum sativum L. Cv. Azad). J. Exp. Bot. 52, 1101–1109.

Du, W., Sun, Y., Ji, R., Zhu, J., Wu, J. and Guo, H., 2011. TiO 2 and ZnO nanoparticles negatively affect wheat growth and soil enzyme activities in agricultural soil. *Journal of Environmental Monitoring*, *13*(4), pp.822-828.

El Far M, Taie HA (2009) Antioxidant activities, total anthocyanins, phenolics and flavonoids contents of some sweetpotato genotypes under stress of different concentrations of sucrose and sorbitol. Aust J Basic Appl Sci 3:3609–3616

El-Batal, A.I., Ismail, M.A., Amin, M.A., El-Sayyad, G.S. and Osman, M.S., 2023. Selenium nanoparticles induce growth and physiological tolerance of wastewater-stressed carrot plants. *Biologia*, pp.1-17.
Elemike, E.E., Fayemi, O.E., Ekennia, A.C., Onwudiwe, D.C. and Ebenso, E.E., 2017. Silver nanoparticles mediated by Costus afer leaf extract: synthesis, antibacterial, antioxidant and electrochemical properties. *Molecules*, *22*(5), p.701.
Elmusa, F., Aygun, A., Gulbagca, F., Seyrankaya, A., Göl, F., Yenikaya, C. and Sen, F., 2021. Investigation of the antibacterial properties of silver nanoparticles synthesized using Abelmoschus esculentus extract and their ceramic applications. *International Journal of Environmental Science and Technology*, *18*, pp.849-860.
El-Shahir AA, El-Tayeh NA, Ali OM et al (2021) The Effect of endophytic Talaromyces pinophilus on growth, absorption and accumulation of heavy metals of Triticum aestivum grown on sandy soil amended by sewage sludge. Plants 10:2659
Gadallah MAA. 1995. Phytotoxic effects of industrial and sewage wastewaters on growth, chlorophyll content, transpiration rate and relative water content of potted sunflower plants. Water Air Soil Poll. 89: 33-47 Burducea, M., Lobiuc, A., Asandulesa, M., Zaltariov, M.F., Burducea, I., Popescu, S.M. and Zheljazkov, V.D., 2019. Effects of sewage sludge amendments on the growth and physiology of sweet basil. *Agronomy*, *9*(9), p.548.
Gill RA, Hu XQ, Ali B, Yang C, Shou JY, Wu YY, Zhou WJ (2014) variation of the responses to chromium toxicity in four oilseed rape cultivars. Biol Plant 58:539–550

Gupta, V.; Mohapatra, S.; Mishra, H.; Farooq, U.; Kumar, K.; Ansari, M.J.; Aldawsari, M.F.; Alalaiwe, A.S.; Mirza, M.A.; Iqbal, Z. Nanotechnology in Cosmetics and Cosmeceuticals—A Review of Latest Advancements. *Gels* **2022**, 8, 173. [CrossRef]

Hasan, M. M., Hossain, S., Poddar, P., Chowdhury, A. A., Katengeza, E. W., & Roy, U. K. (2019). Heavy metal toxicity from the leather industry in Bangladesh: a case study of human exposure in Dhaka industrial area. *Environmental monitoring and assessment, 191(9),* 530.

Hebbalalu, D.; Lalley, J.; Nadagouda, M.N.; Varma, R.S. Greener techniques for the synthesis of silver nanoparticles using plant extracts, enzymes, bacteria, biodegradable polymers, and microwaves. *ACS Sustain. Chem. Eng.* **2013**, 1, 703–712. [CrossRef]

Hsu, Y. T., & Kao, C. H. (2003). Role of abscisic acid in cadmium tolerance of rice (*Oryza sativa L.*) seedlings. *Plant, Cell & Environment, 26*, 867–874. doi:10.1046/j.1365-3040.2003.01018.x.
Hussain, F., Hadi, F. and Rongliang, Q., 2021. Effects of zinc oxide nanoparticles on antioxidants, chlorophyll contents, and proline in Persicaria hydropiper L. and its potential for Pb phytoremediation. *Environmental Science and Pollution Research*, *28*, pp.34697-34713.
Ibrahim MH, Chee KY, Zain M, Amalina NA (2017) Effect of cadmium and copper exposure on growth, secondary metabolites and antioxidant activity in the medicinal plant Sambung Nyawa (Gynura procumbens (Lour.) Merr). Molecules 22:16–23

Kalashgarani, M.Y.; Babapoor, A. Application of nano-antibiotics in the diagnosis and treatment of infectious diseases. *Advan. Appl. NanoBio-Technol*. **2022**, 3, 22–35.

Karthik, C., Barathi, S., Pugazhendhi, A., Ramkumar, V.S., Thi, N.B.D., Arulselvi, P.I., 2017a. Evaluation of Cr(VI) reduction mechanism and removal by *Cellulosimicrobium funkei* strain AR8, a novel haloalkaliphilic bacterium. J. Hazard. Mater. 333, 42e53.

Khan, N. and Bano, A., 2016. Role of plant growth promoting rhizobacteria and Ag-nano particle in the bioremediation of heavy metals and maize growth under municipal wastewater irrigation. *International Journal of Phytoremediation*, *18*(3), pp.211-221.

Kuhn, R.; Bryant, I.M.; Jensch, R.; Böllmann, J. Applications of Environmental Nanotechnologies in Remediation,Wastewater Treatment, DrinkingWater Treatment, and Agriculture. *Appl. Nano* **2022**, 3, 54–90. [CrossRef]

Kumar V, Shahi S, Singh S (2018) Bioremediation: an eco-sustainable approach for restoration of contaminated sites. In Microbial bioprospecting for sustainable development. Springer, pp 115–136

Kuppusamy, S., Thavamani, P., Venkateswarlu, K., Lee, Y.B., Naidu, R., Megharaj, M., 2017. Remediation approaches for polycyclic aromatic hydrocarbons (PAHs) contaminated soils: technological constraints, emerging trends and future directions. Chemosphere 168, 944e968.

Lyubenova, L. and Schröder, P., 2011. Plants for waste water treatment–effects of heavy metals on the detoxification system of Typha latifolia. *Bioresource Technology*, *102*(2), pp.996-1004.

Madamsetty, V.S.; Mukherjee, A.; Mukherjee, S. Recent trends of the bio-inspired nanoparticles in cancer theranostics. *Front. Pharmacol*. **2019**, 3, 1264. [CrossRef]

Mofolo, M.J., Kadhila, P., Chinsembu, K.C., Mashele, S. and Sekhoacha, M., 2020. Green synthesis of silver nanoparticles from extracts of Pechuel-loeschea leubnitziae: their anti-proliferative activity against the U87 cell line. *Inorganic and Nano-Metal Chemistry*, *50*(10), pp.949-955.

Mohammadkhani, N. and Heidari, R., 2008. Drought-induced accumulation of soluble sugars and proline in two maize varieties. *World Appl. Sci. J*, *3*(3), pp.448-453.

Mondal, S. and Chakraborty, K., 2020. Brassicaceae plants response and tolerance to salinity. The Plant Family Brassicaceae: *Biology and Physiological Responses to Environmental Stresses*, pp.203-228.

Monni, S., Uhlig, C., Hansen, E., & Magel, E. (2001). Ecophysiological responses of *Empetrum nigrum* to heavy metal pollution. *Environmental Pollution, 112*, 121– 129. doi:10.1016/S0269-7491(00)00125-1.

Nićiforović N, Mihailović V, Mašković P, Solujić S, Stojković A, Muratspahić DP (2010) Antioxidant activity of selected plant species; potential new sources of natural antioxidants. Food Chem Toxicol 48:3125–3130

Ohta, S.; Mitsuhashi, K.; Chandel, A.K.S.; Qi, P.; Nakamura, N.; Nakamichi, A.; Yoshida, H.; Yamaguchi, G.; Hara, Y.; Sasaki, R. Silver-loaded carboxymethyl cellulose nonwoven sheet with controlled counterions for infected wound healing. *Carbohydr. Polym*. **2022**, 286, 119289. [CrossRef].

Oyiga, B.C.; Sharma, R.; Shen, J.; Baum, M.; Ogbonnaya, F.; Léon, J.; Ballvora, A. Identification and characterization of salt tolerance of wheat germplasm using a multivariable screening approach. *J. Agron. Crop Sci.* **2016**, *202*, 472–485. [Google Scholar] [CrossRef]

Panigrahi, T. Synthesis and characterization of silver nanoparticles using leaf extract of *Azadirachta indica. Appl. NanoBio-Technol*. **2013**, 3, 11–17.

Patsikka, E., Kairavuo, M., Sersen, F., Aro, E.-M., & Tyystjarvi, E. (2002). Excess copper predisposes photosystem II to photoinhibition in vivo by outcompeting iron and causing decrease in leaf chlorophyll. *Plant Physiology, 129*, 1359–1367. doi:10.1104/pp.004788.

Prabhavathi R, Prasad M, Jayaramu M (2016) Studies on qualitative and quantitative phytochemical analysis of Cissus quadrangularis. Adv Appl Sci Res 7:11–17

Radotic, K., T. Ducic and D. Mutavdzic: Changes in peroxidase activity and isozymes in spruce needles after exposure to different concentrations of cadmium. Env iron. Exp. Bot., 44, 105-113 (2000).

Rahman Z, Singh VP (2019) The relative impact of toxic heavy metals (THMs) (arsenic (As), cadmium (Cd), chromium (Cr)(VI), mercury (Hg), and lead (Pb)) on the total environment: an overview. Environ Monit Assess 191:419

Rai, P.K., Yadav, P., Kumar, A., Sharma, A., Kumar, V. and Rai, P., 2022. Brassica juncea: A Crop for Food and Health. *In The Brassica juncea Genome* (pp. 1-13). Cham: Springer International Publishing.

Reddy, N.V., Li, H., Hou, T., Bethu, M.S., Ren, Z. and Zhang, Z., 2021. Phytosynthesis of silver nanoparticles using Perilla frutescens leaf extract: Characterization and evaluation of antibacterial, antioxidant, and anticancer activities. *International journal of nanomedicine*, pp.15-29.

Rong Guo, T., Guo Ping, Z., & Yan Hua, Z. (2007). Physiological changes in barley plants under combined toxicity of aluminum, copper and cadmium. *Colloids and Surfaces. B, Biointerfaces, 57*, 182–188. doi:10.1016/j.colsurfb.2007.01.013.

Sadak, M.S., 2019. Impact of silver nanoparticles on plant growth, some biochemical aspects, and yield of fenugreek plant (Trigonella foenum-graecum). *Bulletin of the National Research Centre*, *43*(1), pp.1-6.

Salehi, B., Quispe, C., Butnariu, M., Sarac, I., Marmouzi, I., Kamle, M., Tripathi, V., Kumar, P., Bouyahya, A., Capanoglu, E. and Ceylan, F.D., 2021. Phytotherapy and food applications from Brassica genus. *Phytotherapy research, 35*(7), pp.3590-3609.

Shahid M, Khalid S, Abbas G et al (2015) Heavy metal stress and crop productivity. Crop production and global environmental issues. Springer, Berlin, pp 1–25

Shahid M, Shamshad S, Rafiq M, Khalid S, Bibi I, Niazi NK, Dumat C, Rashid MI (2017) Chromium speciation, bioavailability, uptake, toxicity and detoxification in soil-plant system: a review. Chemosphere 178:513–533

Shahid M, Shamshad S, Rafiq M, Khalid S, Bibi I, Niazi NK, Dumat C, Rashid MI (2017) Chromium speciation, bioavailability, uptake, toxicity and detoxification in soil-plant system: a review. Chemosphere 178:513–533

Sharma, P., Bhatt, D., Zaidi, M.G.H., Saradhi, P.P., Khanna, P.K. and Arora, S., 2012. Silver nanoparticle-mediated enhancement in growth and antioxidant status of Brassica juncea. *Applied biochemistry and biotechnology*, *167*, pp.2225-2233.

Singh, A. and Agrawal, M., 2010. Effects of municipal waste water irrigation on availability of heavy metals and morpho-physiological characteristics of Beta vulgaris L. *Journal of Environmental Biology*, *31*(5), p.727.

Song, C.; Ye, F.; Liu, S.; Li, F.; Huang, Y.; Ji, R.; Zhao, L. Thorough utilization of rice husk: Metabolite extracts for silver nanocomposite biosynthesis and residues for silica nanomaterials fabrication. *New J. Chem.* **2019**, 43, 9201–9209. [CrossRef]

Sumanta N, Haque CI, Ni shika J , Suprakash R (2014) Spectrophotometric analysis of chlorophylls and carotenoids from commonly grown fern species by using various extracting solvents. Res J Chem Sci 4:63–69

Thombre, R., Mehta, S., Mohite, J. and Jaisinghani, P., 2013. Synthesis of silver nanoparticles and its cytotoxic effect against THP-1 cancer cell line. *International Journal of Pharma and Bio Sciences*, *4*(1), 184-192.

Tiri, R.N.E.; Gulbagca, F.; Aygun, A.; Cherif, A.; Sen, F. Biosynthesis of Ag–Pt bimetallic nanoparticles using propolis extract: Antibacterial effects and catalytic activity on NaBH4 hydrolysis. *Environ. Res*. **2022**, 206, 112622. [CrossRef]

Ullah, A., Heng, S., Munis, M.F.H., Fahad, S., Yang, X., 2015. Phytoremediation of heavy metals assisted by plant growth promoting (PGP) bacteria: a review. Environ. Exper. Bot. 117, 28e40.

Yan, A., Wang, Y., Tan, S.N., Mohd Yusof, M.L., Ghosh, S. and Chen, Z., 2020. Phytoremediation: a promising approach for revegetation of heavy metal-polluted land. *Frontiers in Plant Science, 11*, p.359.

Zafar H, Ali A, Ali JS, Haq IU, Zia MJ (2016) Effect of ZnO nanoparticles on Brassica nigra seedlings and stem explants: growth dynamics and antioxidative response. Front Plant Sci 7:535

Zeraatkar, A.K., Ahmadzadeh, H., Talebi, A.F., Moheimani, N.R., McHenry, M.P., 2016. Potential use of algae for heavy metal bioremediation, a cr